

Evaluation of Cobalt Free Coatings as Hardfacing Material Candidates in Sodium Fast Reactor and Effect of Oxygen in Sodium on the Tribological Behaviour

F.Rouillard¹, B. Duprey¹, J.L. Courouau¹, R. Robin¹, L. Nicolas¹, P. Aubry², C. Blanc²,
M. Tabarant², H. Maskrot², M. Blat-Yriex³, G. Rolland³, T. Marlaud⁴

¹CEA, DEN, DPC, SCCME, LECNA, Université Paris Saclay, France

²CEA, DEN, DPC, SEARS, LISL, Université Paris Saclay, France

³EDF R&D

⁴AREVA NP

E-mail contact of main author: fabien.rouillard@cea.fr

Abstract. The feedback produced by operating Sodium Fast Reactors has shown the importance of material tribological properties. Where galling or adhesive wear cannot be allowed, hardfacing alloys, known to be galling-resistant coatings, are usually applied on rubbing surfaces. The most used coating is the cobalt base alloy named Stellite because of its outstanding friction and wear behavior. Nevertheless, cobalt is an element which activates in the reactor leading to complex management of safety during reactor maintenance and decommissioning. As a consequence, a collaborative work between CEA, EDF and AREVA has been launched for selecting promising cobalt free hardfacing alloys for the 600 MW sodium-cooled fast breeder reactor project named ASTRID. Several nickel base alloys have been selected from literature review then deposited through Plasma Transferred Arc or Laser Cladding on 18Cr austenitic stainless steel 316L(N) according to RCC-MRx Code (AFCEN Code). Among the numerous properties required for qualifying their use as hardfacing alloys in SFR, good corrosion behaviour and good friction and wear behaviour in sodium are essential. The first results obtained on these properties are shown in this article. First, the corrosion behaviour of all coatings was evaluated through exposure tests in purified sodium for 5000 h at 400 °C. Then, the degradation of the surface was carefully appreciated thanks to several complementary analytical techniques. Finally, the friction and wear properties of all candidates were studied in sodium in a dedicated designed facility. The influences of the oxygen concentration in sodium on these properties were evaluated.

Key Words: hardfacing coatings, sodium, Stellite, friction coefficient

1. Introduction

Several zones in the sodium fast reactors (SFR) are in contact and undergo friction during reactor lifetime. The main examples are the insertion and remove of the assembly feet in their candles during fuel replacement or the movement of control rods into the reactor core during operation. During these operations, excellent friction coefficient and very low wear of the components are necessary. Beyond these properties, it is also necessary that the used materials have good compatibility in sodium, good mechanical behavior, metallurgical stability, irradiation resistance, etc. Many studies have been carried out since the 1950s to determine the best possible pairs of material for all applications. The design of SFR prototypes has led to develop specific installations in order to measure the friction coefficient of pairs of materials and to evaluate wear during friction in sodium. The tribological behaviour of tens pairs of materials was evaluated as function of temperature [1], contact stress, roughness [1, 2], sliding rate [1, 3], irradiation [4], oxygen content in sodium [1, 5] and other parameters. From this “material screening”, feedbacks have shown that tribological hard coatings are most of the time necessary in order to limit the wear of the components and

prevent them from jamming or blocking. Stellite 6, a cobalt-base alloy containing hard phases, has been the most widely used coating SFRs. Unfortunately, this alloy has the disadvantage of activating into high energy gamma emitter ^{60}Co hence leading to problems during maintenance and dismantling. As a consequence, research program on several hard nickel-base alloy coatings has been launched. First, their corrosion behaviour in purified sodium at 400 °C was studied up to 5000 h exposure time. Then, in order to study their tribological behavior in sodium, a low scale sodium facility dedicated to tribological studies was developed at CEA/Saclay. The results obtained during the friction of 316L(N) – 316L(N) and 316 L(N) – NiCrBSi alloy contacts in sodium at 200 °C were analyzed. Finally, study of the influence of the oxygen concentration in sodium on the tribological behavior was carried out.

2. Materials and experimental procedure

Sodium preparation: The corrosion test was carried out into 2.4 L static sodium bath contained in molybdenum crucible. In order to limit the pollution of sodium by oxygen during manipulation and during test, the crucible was positioned in a nickel base alloy reactor and subsequently placed in a glove box flushed by high purity argon. The oxygen level in the sodium bath was decreased below 1 ppm in order to be as close as possible to the steady-state oxygen concentration found into running SFRs' sodium (< 10 ppm) [6, 7]. For this purpose, after sodium skimming, zirconium getter foil was inserted into the sodium bath then heated to 600 °C for several days in order to pump out any dissolved oxygen in sodium. Once the sodium purification step was done, the coated specimens were put into the sodium bath with new zirconium getter foil in order to ensure that the oxygen level keeps low for the whole duration of the corrosion test.

Samples and analytical techniques: 2 mm thick hardfacing alloys were coated on one single side of 316L(N) steel grade specimens (25 mm x 20 mm x 3 mm) and exposed into purified liquid sodium at 400 °C for 500 h, 1000 h, 3000 h and 5000 h. The composition of the alloy powders and the processes used for making the coatings are given in TABLE 1. The arithmetic average roughness R_a of the coating surface was measured below 0.4 μm . After immersion, the coupons were cleaned from sodium residues with the same well-controlled procedure in order to have as much as possible the same cleaning process for all samples: in pure ethanol, then in water and then again in pure ethanol for 20 min in an ultrasonic bath. Sample weight variation method was used for evaluating and ranking the corrosion resistance of all samples (mass difference error assessed to be 0.01 mg/cm^2). Finally, the samples were characterized by optical and field emission scanning electron microscopy (FESEM). Modification of the surface composition at the sub-micron scale was carefully followed by Glow Discharge Optical Emission Spectroscopy (GDOES).

TABLE I: WEIGHT CHEMICAL COMPOSITION OF MAIN ALLOYED ELEMENTS OF THE COATING (DEPOSITED METAL).
PTA = PLASMA TRANSFERRED ARC

Harfacing alloy	Process	Base	Cr	C	other	Si	B
CoCrW (eq. Stellite 6)	PTA	Co	28.3	1.1	W: 4.7	1.1	0.0025
	Laser	Co	28.1	1.2	W: 4.8	1.3	/
NiCrBSi A	PTA	Ni	12.7	0.4	B: 2.1	3.4	2.1
NiCrBSi A	Laser	Ni	12.6	0.3	B: 2.2	3.5	2.2
NiCrBSi B	PTA	Ni	12.7	0.4	B:1.8	3.3	1.8
NiMoCrSi	PTA	Ni	15.5	0.04	Mo: 32.7	3.4	/
NiCrSiWB	PTA	Ni	9.6	0.7	W: 1.9 B: 0.5	5.0	0.5

3. Tribological facility and tribological test procedure

In-sodium friction and wear tests were carried out using a plate - plate uniaxial reciprocating-type tribometer similar to the one presented in [8]. The two outer specimens (diameter of 5 mm) were made in 316L(N) steel grade for all friction tests and the central specimen was made of two back to back positioned coated or non-coated 316L(N) samples. The two outer specimens were pressed against the central specimens by lever arms with the load applied by weights. During the friction test, the central specimen was moved up and down by the central pull rod. The friction force was recorded by a load cell and the dynamic friction coefficient μ were calculated by using equation: $\mu = \frac{F_T}{F_N}$ with F_T , the friction force and F_N , the normal force in Newtons. The normal applied force was accurately calibrated before tests thanks to in-situ load-cells positioned in place of the outer specimens. The measurement uncertainty on the applied force given in TABLE II was estimated to be around 10 %. Friction tests were carried out on 316L(N) – 316L(N) and 316L(N) – NiCrBSi alloy B (PTA) contacts. The test parameters are detailed in TABLE II. In order to evaluate the influence of the oxygen concentration in sodium on the tribological behaviour of the tested materials, tests in purified and non-purified sodium were carried out. In the purified sodium test, the specimens were heated in sodium containing zirconium strip at 600 °C for 3 days then cooled down at 200 °C for running the friction test. The oxygen concentration in sodium was estimated below 1 ppm [5, 9]. In the non-purified sodium, the same procedure was carried out but without any zirconium strip. The oxygen concentration in the sodium bath for these tests was estimated between 10 and 20 ppm through sodium purification by zirconium getter foil after test.

TABLE II: FRICTION TESTS
Purified sodium = [O] < 1 ppm ; Non purified sodium = [O] > 10 ppm

Central specimens	Outer specimens	Environment	Operating temperature (°C)	Contact stress (MPa)	Rubbing speed (mm/s)	Rubbing distance (m)
316L(N)	316L(N)	Argon	200	31	1	4
316L(N)	316L(N)	Purified sodium	200	31	1	4
NiCrBSi alloy B (PTA)	316L(N)	Purified sodium	200	31	1	4
NiCrBSi alloy B (PTA)	316L(N)	Non purified sodium	200	31	variable	4

4. Corrosion results and discussion

The mass evolution of the coated samples after 5000 h at 400 °C in purified sodium is shown in FIG. 1. Almost all samples lost mass with time. Nevertheless, for all samples, these mass losses were very low: lower than an equivalent 20 nm thick dissolved nickel layer (except for NiCrBSi alloy A deposited by laser). The strongest mass evolution was observed for NiCrBSi alloy A and B and the lowest for the cobalt-base hardfacing alloy, Stellite 6. After a 5000 h test, the coating process did not appear to have a strong influence on the corrosion behaviour. These low mass evolutions were in good agreement with the low surface alteration observed macroscopically: the samples still appeared metallic colored with the initial machining traces visible on their surface.

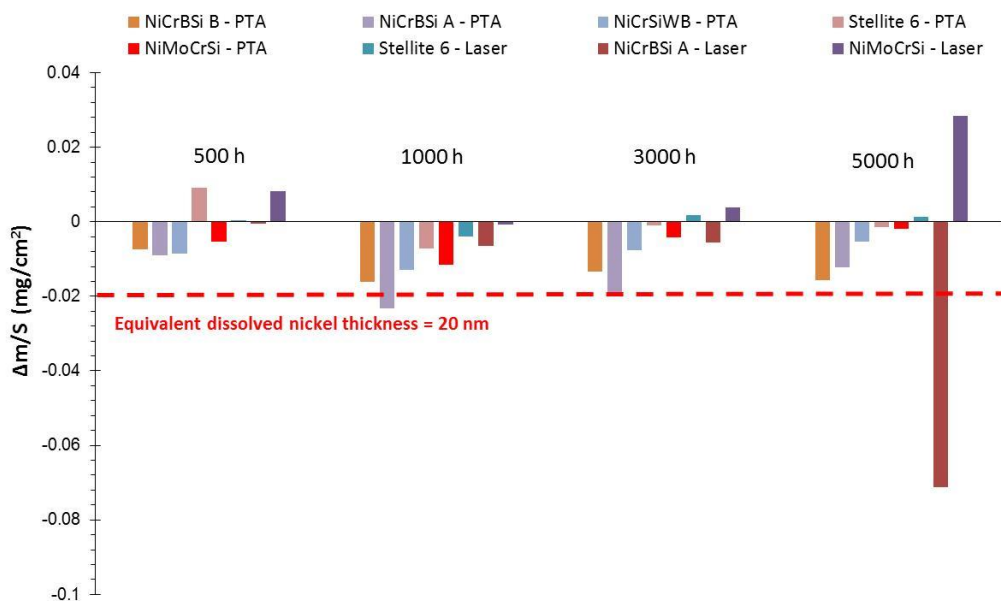


FIG. 1. Mass evolution ($m(t)-m_0$) of the coated samples after 5000 h at 400 °C in purified sodium – [O] < 1 ppm

Nevertheless, FESEM images revealed the formation of a degraded surface layer which thickness varied with the alloy grade. FIG 2. shows the strongest degradation on NiCrBSi alloy A (PTA) after exposure at 400 °C for 5000 h with the formation of 1 μm thick porous zone.

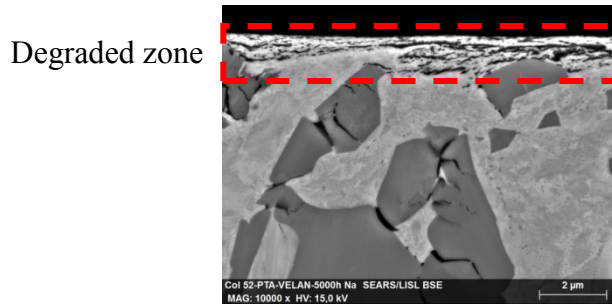


FIG. 2. FESEM image of NiCrBSi alloy A (PTA) cross section surface after exposure in sodium at 400 °C for 5000 h.

For all specimens, the composition of these four elements appeared to vary on the surface: Si, B, Cr and Na. FIG 3. to 6. show the elementary composition evolution of NiCrBSi alloy B, Stellite 6, NiCrSiW and NiMoCrSi surfaces deposited by PTA on 316L(N) steel after exposure at 400 °C for 5000 h in sodium.

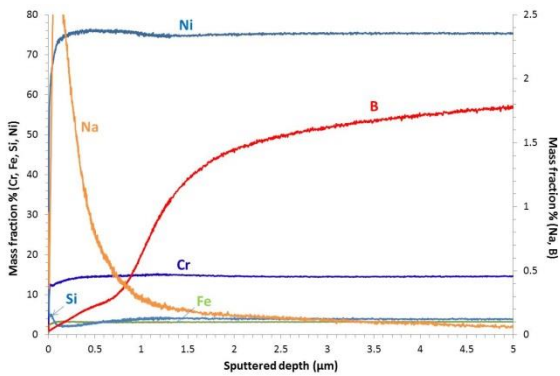


FIG. 3 : Elementary profile of NiCrBSi alloy B (PTA) surface after exposure in Na at 400 °C for 5000 h measured by GDOES

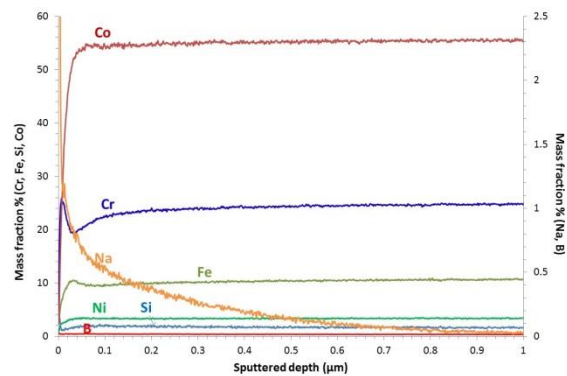


FIG. 4 : Elementary profile of Stellite 6 (PTA) surface after exposure in Na at 400 °C for 5000 h measured by GDOES

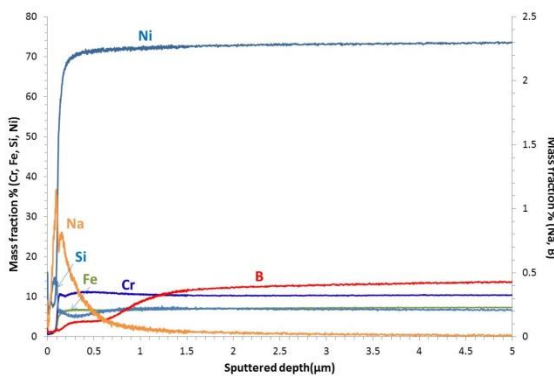


FIG. 5 : Elementary profile of NiCrSiWB alloy (PTA) surface after exposure in Na at 400 °C for 5000 h measured by GDOES

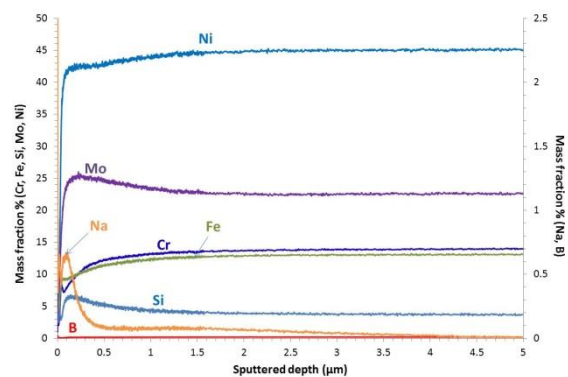


FIG. 6 : Elementary profile of NiMoCrSi alloy (PTA) surface after exposure in Na at 400 °C for 5000 h measured by GDOES

Boron is strongly depleted on the surface of the boron rich coatings NiCrBSi alloys A/B and NiCrSiWB alloy whatever the deposition process (PTA or laser). The boron depleted zone depth increased with time. Boron dissolution in sodium has already been observed for austenitic steels at 600 and 700 °C by Borgstedt et al. [10]. This phenomenon was likely due to boron activity gradient between coatings and sodium. Unfortunately, boron solubility in sodium is unknown [11]. The apparent diffusion coefficient of boron was calculated from the boron depleted profiles and was found to be around 10^{-15} cm²/s. From this diffusion coefficient, the maximum boron depleted zone thickness was evaluated to be below 50 µm after 60 years at 400 °C.

Silicon is the other element which concentration was observed to be depleted at the surface of NiCrBSi and NiCrSiWB coatings whatever the deposition process. The silicon depleted zone was always sodium enriched. Its thickness was related to the one where porosity formation was observed (FIG 2). This coupled sodium – silicon concentration evolution on the surface of alloys after sodium exposure has been often observed in corrosion studies in high temperature liquid sodium. The proposed scenario is that silicon and silica are dissolved into sodium through the formation of soluble sodium silicate NaSi₂O₅ [11] leaving sodium filled pores in the alloy. The solubility of Si in sodium was estimated around 100 ppm at 400 °C [11]. No silicon depletion was observed for NiMoCrSi alloy and Stellite 6 in spite of the fact that they contained 3 - 4 wt% and 1 wt% of Si respectively. This discrepancy for the silicon dissolution rate as function of alloy grade could be attributed to phase dependent silicon dissolution rate. In NiCrBSi type coating, silicon was contained mainly in Ni₃Si phases whereas it was mainly present in the (Ni,Si)₂(Mo,Cr) Laves phases in NiMoCrSi alloy. The hypothetical slower dissolution rate of silicon from Laves phases in NiMoCrSi alloy should be further investigated.

Besides, for all coatings, a chromium depleted zone was observed at the surface. Sometimes, this chromium depleted zone was accompanied by a chromium enriched zone at the sodium – coating interface as observed for Stellite 6 (FIG.4). This enrichment of chromium and its underlying depletion could reveal the formation of NaCrO₂ on the coating surface. This ternary oxide is known to be stable at low oxygen concentration in sodium. Nevertheless its presence could not be demonstrated by XRD even using grazing angle which means that if formed, its amount on the surface were very low.

Finally, sodium penetration was detected through the coating surface. Its penetration depth and its quantity were believed to be strongly linked to the density and depth of cracks and porosity formed on the coating surface during the process. The deepest penetration depth (about 15 µm) and the highest sodium concentration were measured for the NiCrBSi type coatings. This penetration depth was in good agreement with the highest density of cracks on their surface (FIG. 7 and 8). The sodium penetration depth was only around 2 µm for Stellite 6 in good agreement with the absence of visible cracks on its surface. The influence of sodium penetration on the tribological properties in sodium is unknown and should also be investigated.

In conclusion, all tested hardfacing alloys showed good compatibility in purified sodium at 400 °C up to 5000 h exposure time. This observation confirmed literature data indicating corrosion rates from 0.02 µm to 0.1 µm/year for these alloy grades in flowing sodium at 400 °C [12]. The best corrosion behavior in sodium was observed for Stellite 6 and NiMoCrSi alloy and the most reactive alloy was the NiCrBSi type alloys in agreement, again, with literature [13].

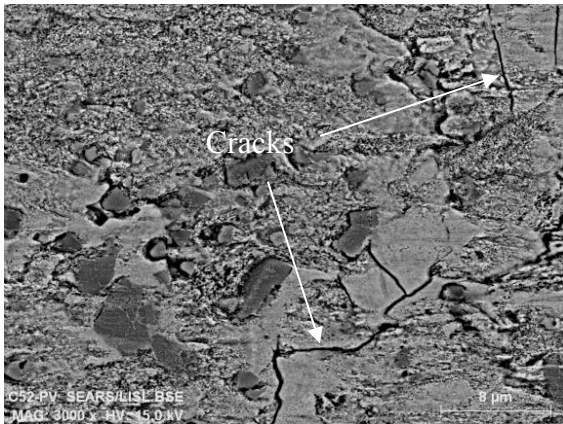


FIG.7 Cracks formed on NiCrBSi alloy A (PTA) surface before exposure in sodium observed by FESEM (surface)

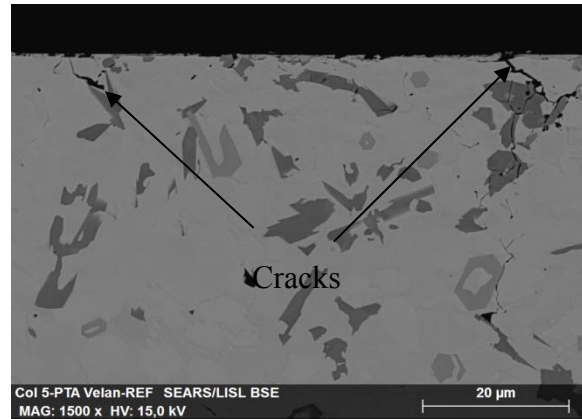


FIG.8 Cracks formed on NiCrBSi alloy A (PTA) surface before exposure in sodium observed by FESEM (cross section)

5. Tribological behavior in sodium

A comparison of the mass evolution of the specimens after friction tests of 316L(N) against itself and 316L(N) against NiCrBSi alloy B (PTA) in purified sodium at 200 °C is shown in FIG 9. The wear resistance of both specimens (central and outer) was much higher when 316L(N) was rubbed against hardfacing alloy NiCrBSi B. Very low mass transfer occurred which contrasted with the 316L(N) – 316L(N) friction test where steel was massively transferred from the outer specimen to the central one (FIG 10). This adhesive wear was also observed when the test was carried out under inert gas. In contrast, the friction coefficient measured during the 316L(N) – NiCrBSi alloy B friction test was almost twice higher than the one measured for the 316L(N) – 316L(N) friction test. No effect of the environment could be observed on the friction coefficient values when comparing the friction test in purified sodium and in argon (FIG 11). This result was in good agreement with the fact that, in both environments, no lubricating oxide layer was formed on the steel surface. This result appeared logical since no lubricating oxide layer was formed on steel surface under both environments.

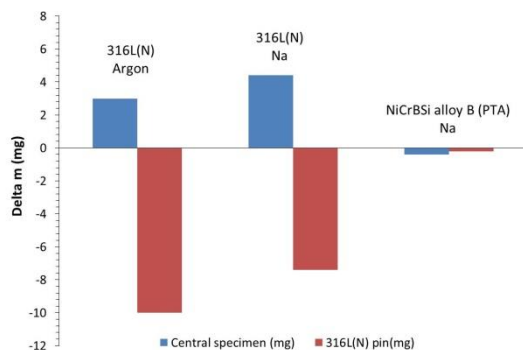


FIG. 9. Mass evolution of pin and central specimens for 316L(N) - 316L(N) friction test in argon and sodium and for 316L(N) – NiCrBSi alloy B (PTA) friction test in sodium at 200 °C under 31 MPa

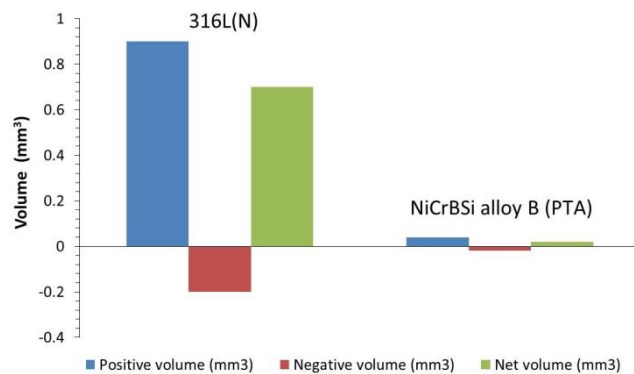


FIG. 10. Positive and negative volumes measured by 3D microscopy on the worn surface of the central specimen after friction test in sodium

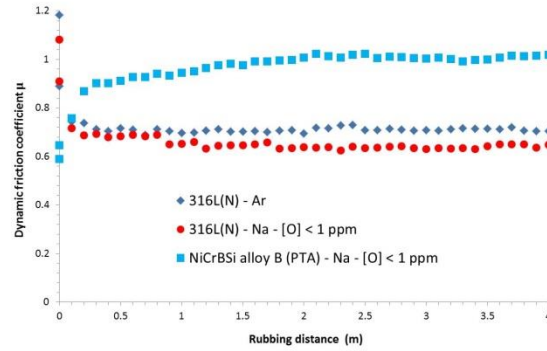


FIG. 11. Dynamic friction coefficient of 316L(N) - 316L(N) and 316L(N) – NiCrBSi alloy B (PTA) contact in purified sodium ($[O] < 1$ ppm) or argon at 200 °C under 31 MPa at 1 mm/s

As it can be seen in FIG. 12, the oxygen concentration in sodium could have an important effect on the tribological behaviour of the two specimens in contact. Indeed, the friction coefficient could be lowered by a factor of 1.5 by increasing the oxygen concentration in sodium from levels below 1 ppm to levels over 10 ppm. This effect has already been observed in past studies and was mainly attributed to the formation of lubricating oxide such as NaCrO_2 on the surface of the steels [2, 5, 14]. This friction coefficient decrease attributed to the formation of an oxide layer well fits with our observation in FIG. 12 revealing that the friction coefficient could be strongly lowered by annealing the specimens in non-purified sodium at 600 °C. During this step, it was very likely that the ternary NaCrO_2 oxide layer formed on the surfaces lowering the friction coefficient to a value equal to 0.3. Then, with increasing rubbing distance, the oxide layer was removed progressively and the friction coefficient increased up to its initial value, around 0.7. Besides, it was observed that the wear resistance of the rubbing contact was slightly improved with the oxygen concentration (FIG 13).

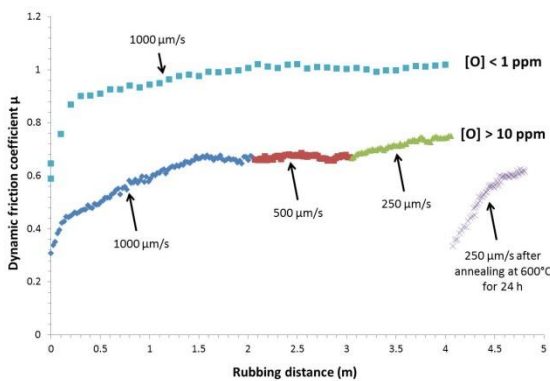


FIG. 12. Dynamic friction coefficient of 316L(N) – NiCrBSi alloy B (PTA) contact in purified ($[O] < 1$ ppm) and non-purified sodium ($[O] > 10$ ppm) at 200 °C under 31 MPa

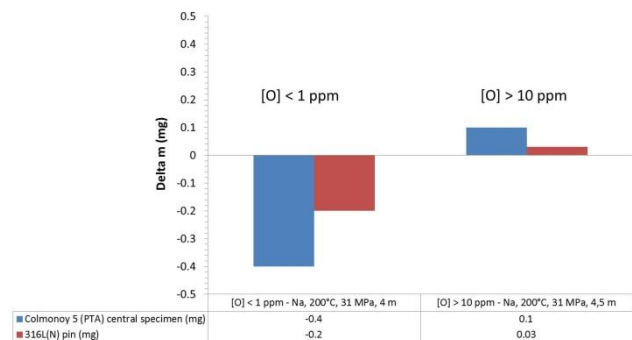


FIG. 13. Mass evolution of pin and central specimens for 316L(N) - NiCrBSi alloy B (PTA) friction test in purified and non-purified sodium at 200 °C under 31 MPa

6. Conclusions

Several nickel-base alloys were evaluated as candidates for hardfacing alloys in SFRs. All of them showed good chemical compatibility in sodium at 400 °C for at least 5000 h, whatever

the deposition process (Plasma Transferred Arc or Laser Cladding). In-sodium friction tests revealed better wear behavior for 316L(N) - NiCrBSi alloy contact than for 316L(N) – 316L(N) contact. However, the measured friction coefficient was higher. The beneficial influence of the oxygen concentration in sodium on the friction coefficient was demonstrated.

7. References

- [1] E. Wild, KJ. Mack and M. Gegenheimer, *Liquid metal tribology in fast breeder reactors*. 1984, Kernforschungszentrum Karlsruhe. p. 151.
- [2] R. N. Johnson, R. C. Aungst, N. J. Hoffman, M. G. Cowgill, G. G. Whitlow and W. L. Wilson, *Proceeding in First international conference on liquid metal technology in energy production*, Champion, ed. M.H. Cooper (1976), p. 122.
- [3] E. Wild, *Friction and wear in liquid-metal systems : compatibility problems of test results obtained from different test facilities*, in *First international conference on liquid metal technology in energy production*. 1976: Champion. p. 131-137.
- [4] G. A. Whitlow, W. L. Wilson, T. A. Galioto, R. L. Miller, S. L. Schrock, N. J. Hoffman, J. J. Droher and R. N. Johnson, *Proceeding in First international conference on liquid metal technology in energy production*, ed. (1976), p. 138-143.
- [5] S. J. Radcliffe, *Proceeding in 7th Leeds-Lyon symposium on Tribology*, Institute of Tribology, ed. D. Dowson (1980), p. 7.
- [6] J. Guidez and B. Bonin, *Réacteurs nucléaires à caloporteur sodium*, (2014).
- [7] J-L. Courouau, F. Balbaud-Célérier, V. Lorentz and T. Dufrenoy, *Proceeding in International Congress on Advances in Nuclear Power Plants (ICAPP '11)*, paper 11152, Nice, France, ed. (2011).
- [8] H. Kumar, V. Ramakrishnan, S. K. Albert, C. Meikandamurthy, B. V. R. Tata and A. K. Bhaduri, *Wear* **270**, (2010).
- [9] H. U. Borgstedt, G. Frees and G. Drechsler, *Werstoffe und Korrosion* **7**, (1970).
- [10] H. U. Borgstedt, G. Frees and H. Schneider, *Nuclear Technology* **34**, (1977).
- [11] Hans Ulrich Borgstedt, Cezary Guminski, Hans Ulrich Borgstedt and Cezary Guminski, *Journal of Physical and Chemical Reference Data* **30**, (2001).
- [12] E. Yoshida, Y. Hirakawa, S. Kano and I. Nihei, *Proceeding in Fourth international conference on liquid metal engineering and technology*, Avignon, ed. SFEN (1988), p. 10.
- [13] S. Kano, *Proceeding in Second International conference on liquid metal and technology in energy production*, Richland, ed. A.N.S.M.S.a.T. Division (1980).

- [14] M. G. Nicholas and I. W. Cavell, *Proceeding in Second international conference on liquid metal technology in energy production*, Richland, Washington., ed. J.M. Dahlke (1980), p. 3-43 ; 3-51.

8. Acknowledgements

This project was supported and funded by CEA, AREVA NP and EDF within the ASTRID project.